Available online at www.sciencedirect.com
ScienceDirect
Journal of Photochemistry and Photobiology A: Chemistry 191 (2007) 97–103
Journal of Photochemistry and Photobiology A:Chemistry
www.elsevier.com/locate/jphotochem

Radiative properties of rare earth complexes/silver nanoparticles nanocomposite

Si Wu, Youyi Sun, Xin Wang, Wenxuan Wu, Xiujie Tian, Qing Yan, Yanhua Luo, Qijin Zhang *

Department of Polymer Science and Engineering, University of Science and Technology of China, Hefei, Anhui 230026, PR China

Received 11 January 2007; received in revised form 15 March 2007; accepted 5 April 2007
Available online 8 April 2007

Abstract

Rare earth complexes/silver nanoparticles nanocomposite was prepared by introducing $Tb(TTA)_3Bipy$ as stabilizer. The radiative properties of the nanocomposite were studied by experiments and spectra calculation. The transmission electron microscope image of the composite indicates that the silver nanoparticles are spherical, monodispersed and with an average size of 18 nm. Fluorescence study shows silver nanoparticles have both enhancement effect and quenching effect on the fluorescence of europium complex, the total effect in such a composite system is an enhancement effect. Theory calculation prognosticates that the newly synthesized rare earth complexes/silver nanoparticles nanocomposite could be used in polymer optical fiber amplifier and laser materials.

Keywords: Fluorescence; Rare earth complex; Silver nanoparticles

1. Introduction

Luminescent rare earth ions have many unusual spectroscopic properties such as sharp emission peaks, long lifetimes, large stocks shifts and high quantum yields, which make them so ideal for laser, phosphor, light-emitting diodes (LED) and fluoroimmunoassay applications [1–6]. Due to the poor absorption, rare earth ions are not used directly but form complexes with organic ligands which act as antennas to absorb light and transfer energy to the rare earth ions. In our previous work, the fluorescence properties of rare earth complexes and their applications in polymer photonics materials (PPM) such as polymer optical fiber laser, polymer optical fiber amplifier and three-dimensional multilayered optical memory materials were studied [7–10]. As we know, the fluorescence efficiency of rare earth complexes is an important parameter with regard to their potential use as PPM [11]. There are many methods to improve the fluorescence efficiency of rare earth complexes, such as using deuterated or fluorinated materials [12,13], adding Lewis base [14,15] and using more suitable ligands [16,17]. However, these methods are based on reducing the rate of non-radiative decays or using more efficient antennas. Another effective strategy is to intensify electromagnetic field around rare earth ions. In this paper, we report the luminescent enhancement of silver nanoparticles on Eu(III) complex in nanocomposite, which have potential application values in PPM.

Pioneering experiments on the luminescent properties of the europium ion located in close proximity to a metallic surface in film materials were done by Drexhage et al. [18,19] and Barnes et al. [20,21], respectively. Selvan et al. [22,23] studied silver nanoparticle/Eu^{3+} doped SiO_2 gels, they found although there is no energy transfer from silver to Eu^{3+}, the fluorescence intensity of Eu^{3+} is enhanced by the intensified electromagnetic field around Eu^{3+}. Although film materials and SiO_2 gels have application values, europium complexes are required in solution phase as luminescent labels for biological applications. With this purpose, Nabika et al. [24] and Louis et al. [25] did fundamental studies on the effect of noble metal nanoparticles on rare earth ions in solution phase. It is known, europium complexes are required to be used in organic monomer solution for PPM fabrication. With the desirability to improve the luminescent efficiency of the rare earth complex and to use

* Corresponding author. Tel.: +86 551 3601 704; fax: +86 551 3601 704.
E-mail address: zqjm@ustc.edu.cn (Q. Zhang).

1010-6030/$ – see front matter © 2007 Elsevier B.V. All rights reserved.
doi:10.1016/j.jphotochem.2007.04.009

the high efficient emitter in PPM, silver nanoparticles coated with rare earth complexes was synthesized by our group [26]. Although there is energy transfer from the silver nanoparticles to the rare earth complex, there is strong fluorescence quenching effect due to the condensed J-aggregation and subsequent concentration quenching. To conquer the quenching effect, another kind of silver nanoparticles was synthesized [27], but the nanoparticles showed a limited stability. The instability is due to the chemical activity of HTTA which is used to stabilize silver nanoparticles as well as modulate the concentration of $Eu(TTA)_3{\cdot}2H_2O$ around silver nanoparticles. HTTA is very sensitive to base due to the active H atom and has strong chelating effect to numerous metal ions due to its β-diketone structure. To conquer the defects above, $Tb(TTA)_3Bipy$ (TTA is α-thenoyltrifluoroacetonato, Bipy is 2,2′-bipyridine) is chosen as the stabilizer in this work, then $Eu(TTA)_3Bipy$ which has strong interaction with silver nanoparticles is added to form nanocomposite. $Tb(TTA)_3Bipy$ is quit stable (TTA does not have active H atom and TTA has already chelated with Tb^{3+}) and it can reduce the degree of the condensed J-aggregation of $Eu(TTA)_3Bipy$ around silver nanoparticles. In this work, the radiative properties of this newly synthesized nanocomposite are studied by spectroscopic experiments and Judd–Ofelt theory.

2. Experiment

Morphology and electron diffraction of the silver nanoparticles were measured on a Hitachi H-800 transmission electron microscope (TEM, Japan). UV–vis absorption spectra were measured on a Shimadzu UV-2501 Spectrophotometer (Japan). The fluorescence spectra were measured on a Shimadzu RF-5301PC Fluorescence Spectrophotometer (Japan). The lifetimes were measured on a FluoroLOG-3-TAU steady-state/lifetime spectrofluorometer.

Synthesis of the rare earth complexes ($RE(TTA)_3Bipy$, the structures were shown in Scheme 1) were described in our previous work [16]. Here, it is important to point out the thiophene group (containing S atom) of TTA leads the rare earth complex has strong interactions with silver nanoparticles. The process of preparing the rare earth complexes/silver nanoparticles nanocomposite is shown in Scheme 2. There are two steps to prepare the rare earth complexes/silver nanoparticles nanocomposite. The first step is to use $NaBH_4$ to reduce $AgNO_3$ in the presence of $Tb(TTA)_3Bipy$. This process is similar to our previous work [26], except for changing $Eu(TTA)_3{\cdot}2H_2O$ to $Tb(TTA)_3Bipy$. The synthesis process is described below. $Tb(TTA)_3Bipy$ (1.2 mmol) and $AgNO_3$ (0.4 mmol) were dissolved in acetone (150 ml) and distilled water (10 ml), respectively. After mixing the two solutions, $NaBH_4$ aqueous solution (20 ml, 0.83 mmol) was dropped into the mixture slowly under vigorous stirring. The reaction solution was left overnight with rapid stirring. Then, centrifuging (3000 rpm) gave a brown precipitates. The precipitates were dissolved into acetone/water again. The purification was repeated for 3 times. Formation of the silver nanoparticles is confirmed by TEM and UV–vis spectra. The second step is to mix the silver nanoparticles and $Eu(TTA)_3Bipy$ under ultrasonic for 1 h. This process is similar to our previous work [27], except for changing HTTA-coated silver nanoparticles to the silver nanoparticles prepared in the first step. The final concentration of silver is 5.1 μg/ml which is suitable for fluorescence enhancement [24,27]. In the paper below, $Ag/Eu(TTA)_3Bipy$ is short for the rare earth complexes/silver nanoparticles nanocomposite.

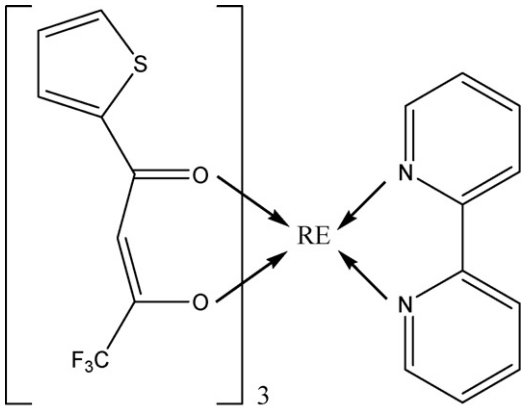

RE= Eu, Tb

Scheme 1. The chemical structures of $Eu(TTA)_3Bipy$ and $Tb(TTA)_3Bipy$.

3. Results and discussion

As shown in Fig. 1a, the silver nanoparticles are almost spherical. The electron diffraction pattern of $Ag/Eu(TTA)_3Bipy$ is shown in the inset of Fig. 1a. Four fringe patterns are (1 1 1), (2 0 0), (2 2 0) and (3 1 1), which indicate the silver nanoparticles are with good crystalline. The size distribution of the silver nanoparticles shown in Fig. 1b indicates the

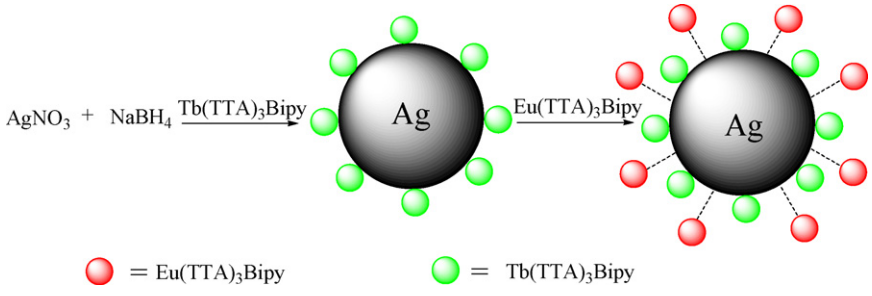

Scheme 2. The process of synthesis of $Ag/Eu(TTA)_3Bipy$.

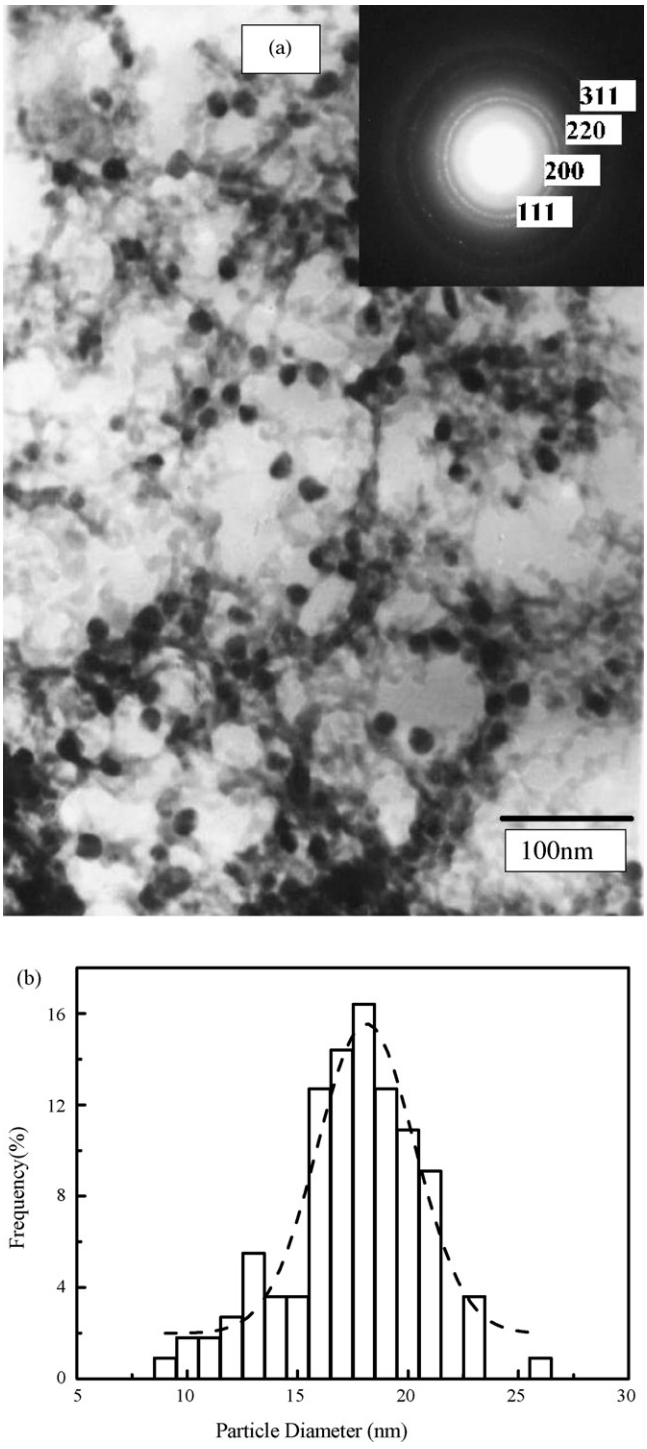

Fig. 1. (a) TEM image of silver nanoparticles (inset is the electron diffraction pattern), (b) size distribution of the silver nanoparticles.

sample is monodispersed and with an average size of 18 nm. Silver nanoparticles with the size of 18 nm are suitable for fluorescence enhancement [24].

Fig. 2 shows the UV–vis spectra of the $Eu(TTA)_3Bipy$, $Ag/Eu(TTA)_3Bipy$ right after synthesized and $Ag/Eu(TTA)_3$ Bipy placed for 6 weeks. As shown in Fig. 2 curve b, formation of silver nanoparticles can be further confirmed by the characteristic plasmon absorption peak of silver nanoparticles which appears at 424 nm [24,26]. There is another strong absorption peak at 343 nm in curve b, which is attribute to the $\pi \rightarrow \pi^*$ transition of the ligands of rare earth complexes. The $\pi \rightarrow \pi^*$ transition absorption peak of the rare earth complex in curve b is red-shifted (about 5 nm) compared with the absorption peak in $Eu(TTA)_3Bipy$ solution (curve a). The red-shift of absorption [26,27]. Compared with $Eu(TTA)_3 \cdot 2H_2O$ coated silver nanoparticles (red-shift 18.2 nm), the red-shift in $Ag/Eu(TTA)_3Bipy$ (5 nm) is much smaller [26], so the J-aggregation is not so condensed. The smaller red-shift reduced the concentration quenching effect (see fluorescence spectra in Fig. 3a and the radiative parameters in Table 2). Compared with curve b, $Ag/Eu(TTA)_3Bipy$ placed for 6 weeks (curve c) does not show significant change, which indicates the silver nanoparticles is quit stable. The stability of the silver nanoparticles is necessary for it to be used in high quality PPM.

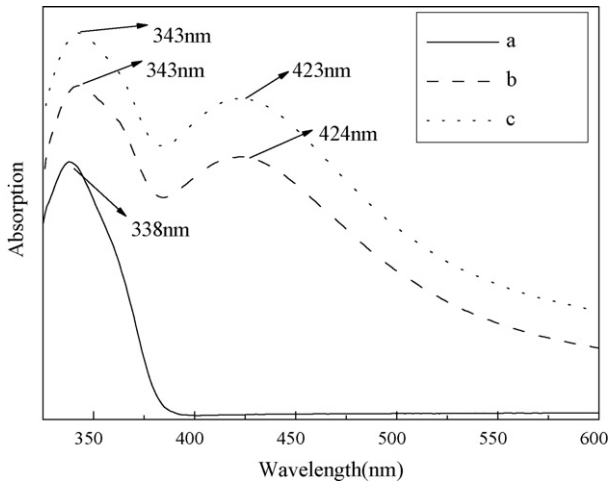

Fig. 2. The UV–vis spectra of (a) $Eu(TTA)_3Bipy$, (b)$Ag/Eu(TTA)_3Bipy$ tested right after synthesized, (c)$Ag/Eu(TTA)_3Bipy$ tested 6 weeks later.

The fluorescence spectra of $Eu(TTA)_3Bipy$ and $Ag/Eu(TTA)_3Bipy$ are shown in Fig. 3a. Five Eu^{3+} characteristic emission peaks which are assignable to $^5D_0 \rightarrow {}^7F_j$ ($j = 0$–4) can be observed. In addition, there is an increment of 21% of the fluorescence intensity of $Ag/Eu(TTA)_3Bipy$ compared with that of $Eu(TTA)_3Bipy$. In our previous work, silver nanoparticles coated with $Eu(TTA)_3 \cdot 2H_2O$ gave a quenched emission due to the condensed J-aggregation and subsequent concentration quenching [26]. After adding $Tb(TTA)_3Bipy$ to reduce the degree of J-aggregation and modulate the concentration of europium complex this time, the quenching effect is not so serious (the red-shift in the UV–vis spectrum is smaller, J-aggregation is not so condensed). There is another deduction form the fluorescence enhancement, that is $Eu(TTA)_3Bipy$ must be near silver nanoparticles, because rare earth complex can be affected by the surface plasmon resonance only when the rare earth complex is near the surface of silver nanoparticles. To confirm our point of view, $Eu(DBM)_3Bipy$ (DBM is dibenzoylmethane, which does not contain S atom so that it does not have interaction with silver nanoparticles) was used as a reference. The fluorescence spectra of $Eu(DBM)_3Bipy$ and $Ag/Eu(DBM)_3Bipy$ are shown in Fig. 3b. Compared with $Eu(DBM)_3Bipy$, there is a decre-

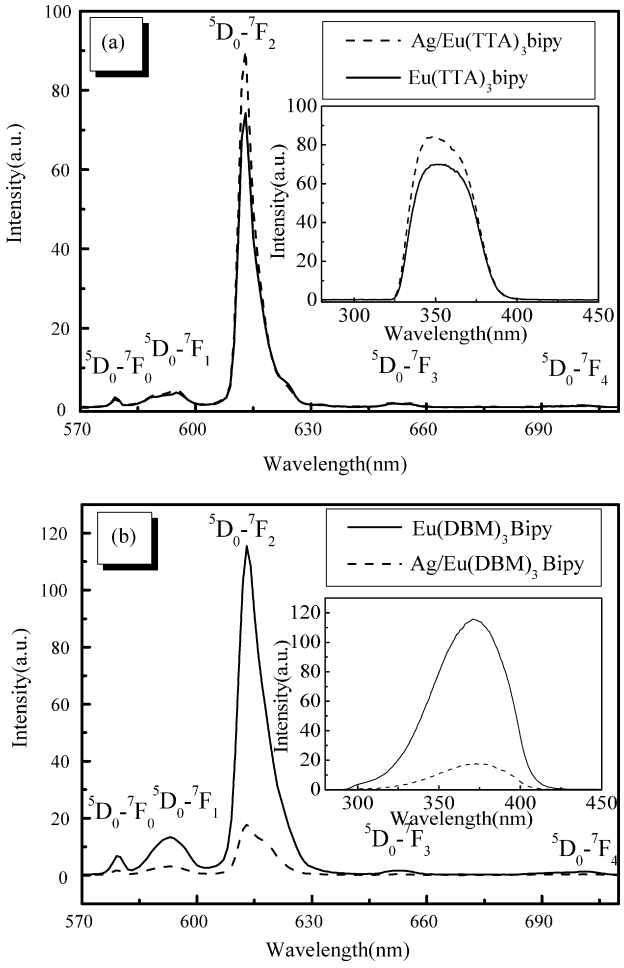

Fig. 3. (a) The fluorescence spectra of Ag/Eu(TTA)$_3$Bipy and Eu(TTA)$_3$Bipy. The inset shows the excitation spectra of Ag/Eu(TTA)$_3$Bipy and Eu(TTA)$_3$Bipy. (b) The fluorescence spectra of Ag/Eu(DBM)$_3$Bipy and Eu(DBM)$_3$Bipy. The inset shows the excitation spectra of Ag/Eu(DBM)$_3$Bipy and Eu(DBM)$_3$Bipy.

ment of 85% of the fluorescence intensity of Ag/Eu(DBM)$_3$Bipy which is due to the quenching effect of silver nanoparticles. Silver nanoparticles also have quenching effect on luminescent rare earth complex because of its absorption, scattering and reflecting [24,27]. The difference between Ag/Eu(TTA)$_3$Bipy and Ag/Eu(DBM)$_3$Bipy is that besides quenching effect, there is fluorescence enhancement effect in Ag/Eu(TTA)$_3$Bipy because Eu(TTA)$_3$Bipy can be affected by the surface plasom resonance. So, the actual fluorescence enhancement by the surface plasom resonance in Ag/Eu(TTA)$_3$Bipy is much bigger than 21%. In Louis's work [25], the luminescence enhancement is found to be greater for the excitation wavelengths corresponding to the maximum of gold nanoparticles absorption. So, the fluorescence enhancement in their system is the antenna effect of gold nanoparticles on the rare earth ion. The fluorescence enhancement mode in our system is quit different. As shown in the excitation spectra of Ag/Eu(TTA)$_3$Bipy (inset of Fig. 3a), the intensity of the excitation corresponding to the maximum of silver nanoparticles absorption (around 424 nm) is nearly 0. So, the fluorescence enhancement is due to the intensified electromagnetic field around Eu^{3+} [23].

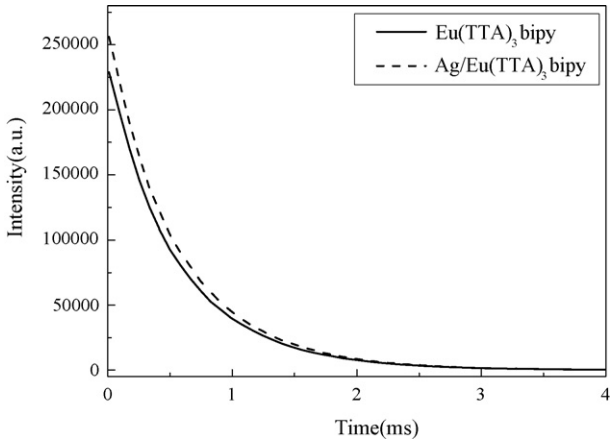

Fig. 4. Fluorescence decay curves of Eu(TTA)$_3$Bipy and Ag/Eu(TTA)$_3$Bipy which were monitored at 613 nm.

Fig. 4 shows the fluorescence decay curve of Ag/Eu(TTA)$_3$ Bipy and Eu(TTA)$_3$Bipy. The lifetimes are shown in Table 1. The lifetimes of Eu(TTA)$_3$·2H$_2$O solution and sliver nanoparticles coated with Eu(TTA)$_3$·2H$_2$O are also listed in Table 1 as references. As shown in Table 1, concentration quenching caused sliver nanoparticles coated with Eu(TTA)$_3$·2H$_2$O had shorter lifetime. Different from the system of sliver nanoparticles coated with Eu(TTA)$_3$·2H$_2$O, the lifetime of Ag/Eu(TTA)$_3$Bipy is no shorter than that of Eu(TTA)$_3$Bipy. That is to say the quenching effect is effectively avoided.

We can also have a better understanding of the interactions between Eu(TTA)$_3$Bipy and Tb(TTA)$_3$Bipy through lifetime study. In other group's work [22,23], they found silver nanoparticles will not affect the lifetime of Eu^{3+}. It is known Tb^{3+} will affect the lifetime of Eu^{3+} if there is energy transfer between them [28]. There is no obvious change in lifetime before and after Eu(TTA)$_3$Bipy adsorbed onto silver nanoparticles. So, the effect of Tb(TTA)$_3$Bipy on Eu(TTA)$_3$Bipy in our system can be negligible.

From what have been discussed above, we can conclude that silver nanoparticles have both enhancement and quenching effect on europium complex, and the total effect in our system is an enhancement effect. Next part is to have a deeper understanding of the radiative properties of Ag/Eu(TTA)$_3$Bipy and prognosticate if Ag/Eu(TTA)$_3$Bipy could be used in high quality photonics materials. Judd–Ofelt theory [29,30] is employed to calculate the radiative parameters of Ag/Eu(TTA)$_3$Bipy and Eu(TTA)$_3$Bipy.

According to Judd–Ofelt theory, the line strength S_{ed} of an electric dipole transition from initial J manifold $|(S, L)J\rangle$ to

Table 1
Luminescence lifetimes

Materials	τ_{decay}(ms) ± 0.001	Data source
Eu(TTA)$_3$Bipy solution	0.609	This work
Ag/Eu(TTA)$_3$Bipy	0.617	This work
Eu(TTA)$_3$·2H$_2$O solution	0.386	Previous work [26]
Eu(TTA)$_3$·2H$_2$O coated silver nanoparticles	0.368	Previous work [26]

terminal manifold $|(S', L')J'\rangle$ can be expressed in terms of three phenomenological parameters, Ω_2, Ω_4, Ω_6 [31,32]:

$$S_{ed} = \sum_{t=2,4,6} \Omega_t |\langle (S, L)J||U^{(t)}||(S', L')J'\rangle|^2 \quad (1)$$

$||U^{(t)}||^2$ are the squared reduced matrix elements of the rank $t = 2, 4, 6$ and their values are not changing with the host for rare earth ions. The $||U^{(t)}||^2$ values of Eu^{3+} are taken form Caird et al. [33]. The three coefficients Ω_2, Ω_4, Ω_6 contain implicitly the odd-symmetry crystal field terms, radial integrals and perturbation denominators.

The Einstein spontaneous emission probability of an electric dipole transition between initial J manifold $|(S, L)J\rangle$ to terminal manifold $|(S', L')J'\rangle$ is given by [31,32]:

$$A_{ed} = A[(S, L)J; (S', L')J'] = \frac{64\pi^4 e^2 \nu^3}{3h(2J+1)} \frac{n(n^2+2)^2}{9} S_{ed}$$
$$= \frac{64\pi^4 e^2 \nu^3}{3h(2J+1)} \frac{n(n^2+2)^2}{9} \times \sum_{t=2,4,6} \Omega_t |\langle (S, L)J||U^{(t)}||(S', L')J'\rangle|^2 \quad (2)$$

h is Plank's constant, n the refractive index of the medium, e the charge of the electron, ν the wavenumber of the transition, J the total angular momentum of the ground state.

It is known that the $^5D_0 \rightarrow {}^7F_1$ transition of Eu^{3+} is magnetic dipole transition which is independent and can be used as a reference. The spontaneous emission probability of the magnetic dipole transition A_{md} is [31,32]:

$$A_{md} = \frac{64\pi^4 \nu^3}{3h(2J+1)} n^3 S_{md} \quad (3)$$

S_{md} refers to the strength of the magnetic dipole line strength of the $^5D_0 \rightarrow {}^7F_1$ transition. It is a constant and independent of the medium.

The total transition emission probability A_T is calculated using [31,32]:

$$A_T = \sum_{S,L,J} A[(S, L)J; (S', L')J'] \quad (4)$$

The fluorescence branching ratio is obtained from:

$$\beta[(S, L)J; (S', L')J'] = \frac{A[(S, L)J; (S', L')J']}{\sum_{S,L,J} A[(S, L)J; (S', L')J']} \quad (5)$$

The radiative lifetime of the transition involved is an important parameter in consideration of the pumping requirement for the threshold of laser action and can be calculated as:

$$\tau_{rad}[(S, L)J] = \frac{1}{\sum_{S,L,J} A[(S, L)J; (S', L')J']} \quad (6)$$

Another important radiative property is the stimulated emission cross section of the measured fluorescence:

$$\sigma[(S, L)J; (S', L')J'] = \frac{\lambda_p^4}{8\pi c n^2 \Delta\lambda_{eff}} A[(S, L)J; (S', L')J'] \quad (7)$$

λ_p is the peak position of the emission line, and $\Delta\lambda_{eff}$ the effective band width of the emission transition.

As shown in Table 2, there is not very big differences between the radiative parameters of Ag/Eu(TTA)$_3$Bipy and Eu(TTA)$_3$Bipy because the electron transition is at 4f energy levels which is protected by the energy levels outside and by the ligands [16]. It is found the radiative parameters reveal the balance between the fluorescence enhancement and quenching by carefully comparing. Ω_2 and β of Ag/Eu(TTA)$_3$Bipy are smaller than those of Eu(TTA)$_3$Bipy, which reveal the quenching effect. On the other hand, the fluorescence intensity and σ of Ag/Eu(TTA)$_3$Bipy are bigger than those of Eu(TTA)$_3$Bipy which reveal the enhancement effect. The balance between the fluorescence enhancement and quenching is attributed to the structure of the nanocomposite. The big concentration of Eu(TTA)$_3$Bipy near silver nanoparticles, the absorption, scattering and reflecting of silver nanoparticles will cause fluorescence

Table 2

Emission transition	ν (cm^{-1})	A_{ed} (s^{-1})	A_{md} (s^{-1})	A (s^{-1})	β (%)	σ (10^{-22} cm^2)
(a) Radiative parameters of Ag/Eu(TTA)$_3$Bipy $\Omega_2 = 17.62 \times 10^{-20}$ cm^2, $\Omega_4 = 0.55 \times 10^{-20}$ cm^2						
$^5D_0 \rightarrow {}^7F_0$	17271	0	0	0	0	0
$^5D_0 \rightarrow {}^7F_1$	16807	0	34.85	34.85	7.98	2.99
$^5D_0 \rightarrow {}^7F_2$	16313	396.23	0	396.23	90.68	67.39
$^5D_0 \rightarrow {}^7F_3$	15337	0	0	0	0	0
$^5D_0 \rightarrow {}^7F_4$	14265	5.87	0	5.87	1.34	0.77
A_T (s^{-1})				436.95		
Radiative lifetime $\tau_{rad} = 2.289$ (ms)						
(b) Radiative parameters of Eu(TTA)$_3$Bipy solution $\Omega_2 = 18.09 \times 10^{-20}$ cm^2, $\Omega_4 = 0.50 \times 10^{-20}$ cm^2						
$^5D_0 \rightarrow {}^7F_0$	17271	0	0	0	0	0
$^5D_0 \rightarrow {}^7F_1$	16807	0	34.85	34.85	7.80	2.86
$^5D_0 \rightarrow {}^7F_2$	16313	406.75	0	406.75	91.00	62.78
$^5D_0 \rightarrow {}^7F_3$	15337	0	0	0	0	0
$^5D_0 \rightarrow {}^7F_4$	14245	5.36	0	5.36	1.20	0.73
A_T (s^{-1})				446.96		
Radiative lifetime $\tau_{rad} = 2.237$(ms)						

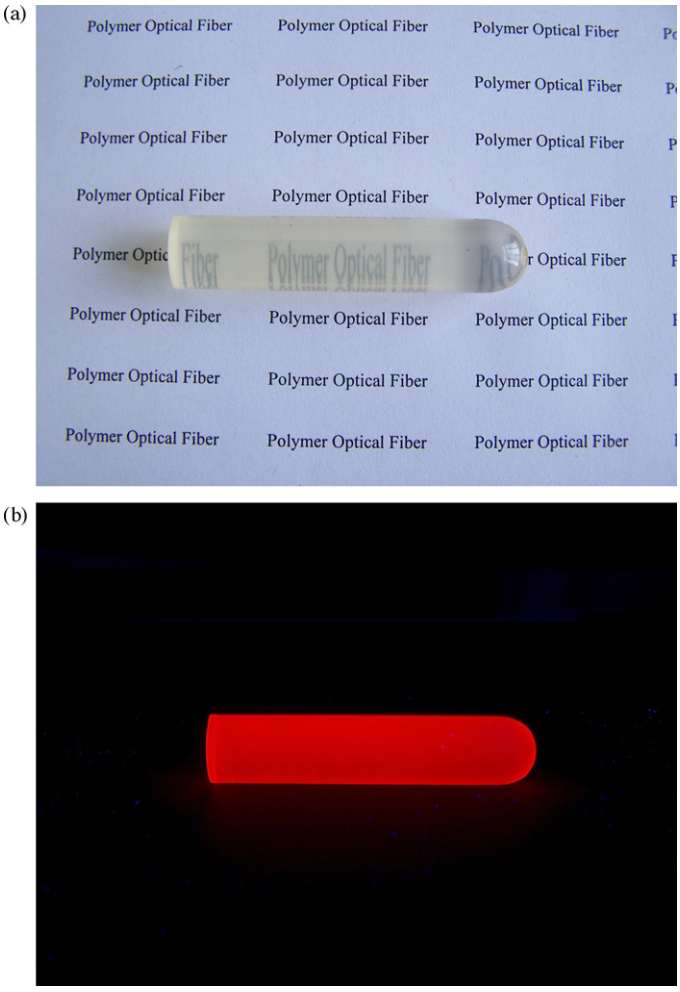

Fig. 5. Colour photographs of Ag/Eu(TTA)$_3$Bipy doped PMMA optical fiber preform in daylight (a) and under 365 nm UV light (b).

quenching [24,27]; the surface plasmon resonance of silver nanoparticles will cause the fluorescence enhancement. So, the calculated radiative parameters can contact the structure of the nanocomposite with the radiative properties. Recent works show noble metal particles will affect the emission process of emitters [34,35]. The increment in stimulated emission cross section in our work indicates silver nanoparticles affects the emission process of Eu(TTA)$_3$Bipy.

The radiative parameters can also prognosticate if the luminescent materials have application values. As shown in Table 2a, the $^5D_0 \rightarrow {}^7F_2$ transition shows the highest β value. It has been established that an emission level with β value bigger or near 50% is a potential laser emission transition [36]. The radiative time is also close to europium benzoylacetonate whose laser phenomena have been reported [15]. Additionally, the stimulated emission cross section of $^5D_0 \rightarrow {}^7F_2$ is 67.39×10^{-22} cm^2, higher than Eu(DBM)$_3$Phen doped PMMA in which optical amplification effect is observed [8]. All these radiative parameters show that the $^5D_0 \rightarrow {}^7F_2$ transition of Ag/Eu(TTA)$_3$Bipy is a possible laser transition and can be used in optical amplification.

Based on the theory calculation that Ag/Eu(TTA)$_3$Bipy have application values in polymer optical fiber laser and polymer optical fiber amplifier, the optical fiber preform is fabricated using Ag/Eu(TTA)$_3$Bipy doped PMMA (poly(methyl methacrylate)). First, Ag/Eu(TTA)$_3$Bipy is dispersed into the monomer (MMA). Then, Ag/Eu(TTA)$_3$Bipy doped MMA was polymerized in a model in a given process. The preform of the polymer optical fiber is quit transparent and uniform. It emits strong red light under UV lamp (see Fig. 5). Silver nanoparticles doped three-dimensional multilayered optical memory materials and nonlinear optical polymer materials can be also fabricated in a process similar to the polymer optical fiber preform.

4. Conclusion

In this paper, rare earth complexes/silver nanoparticle nanocomposite is synthesized. TEM test reveals the silver nanoparticles are monodispersed, good crystalline and the size of the nanoparicles is suitable for fluorescence enhancement. Adding Tb(TTA)$_3$Bipy in the first step to reduce the degree of J-aggregation and modulate the concentration of Eu(TTA)$_3$Bipy has effectively avoided the concentration quenching. Fluorescence study shows silver nanoparticles have both enhancement and quenching effect on the fluorescence of europium complex. The radiative parameters calculated from Judd–Ofelt theory reveals the nanocomposite has potential application values in high-quality photonics materials.

Acknowledgments

This work is supported by the National Natural Science Foundation of China (Grant Nos. 50533040 and 50573071), National Basic Research Program of China (No. 2006cb302900) and Chinese Academy of Sciences (No. kjcx3.syw.H02).

References

[1] V. Bekiari, P. Lianos, Adv. Mater. 10 (1998) 1455.
[2] J. Kido, H. Hayase, K. Hongawa, K. Nagai, Appl. Phys. Lett. 65 (1994) 2124.
[3] F.S. Richardon, Chem. Rev. 82 (1982) 541.
[4] O. Prat, E. Lopez, G. Mathis, Anal. Biochem. 195 (1991) 283.
[5] M.D. McGehee, T. Bergstedt, C. Zhang, A.P. Saab, M.B. O'Regan, G.C. Bazan, V.I. Srdanov, A.J. Heeger, Adv. Mater. 11 (1999) 1349.
[6] A.K. Saha, K. Kross, E.D. Kloszewski, D.A. Upson, J.L. Toner, R.A. Snow, C.D.V. Black, V.C. Desai, J. Am. Chem. Soc. 115 (1993) 11032.
[7] Q. Zhang, P. Wang, X. Sun, Y. Zhai, P. Dai, B. Yang, H. Ming, J. Xie, Appl. Phys. Lett. 72 (1998) 407.
[8] H. Liang, Z. Zheng, Q. Zhang, H. Ming, Z. Li, J. Xu, B. Chen, H. Zhao, Optics Lett. 29 (2004) 477.
[9] H. Jiu, H. Tang, J. Zhou, J. Xu, Q. Zhang, H. Xing, W. Huang, A. Xia, Optics Lett. 30 (2005) 774.
[10] J. Ding, H. Jiu, J. Bao, J. Lu, W. Gui, Q. Zhang, C. Gao, J. Comb. Chem. 7 (2005) 69.
[11] K. Kuriky, Y. Koike, Y. Okamoto, Chem. Rev. 102 (2002) 2347.
[12] K. Kuriki, S. Nishihara, Y. Nishizawa, A. Tagaya, Y. Okamoto, Y. Koike, Electron. Lett. 37 (2001) 415.
[13] T. Kobayashi, K. Kuriki, S. Nakatsuka, Y. Okamoto, Y. Koike, Proc. SPIE 3942 (2000) 158.
[14] M. Kleinerman, R.J. Hovey, D.O. Hoffman, J. Chem. Phys. 41 (1964) 4009.
[15] T. Kobayashi, K. Kuriki, N. Imai, T. Tamura, K. Sasaki, Y. Koike, Y. Okamoto, Proc. SPIE 3623 (1999) 206.

[16] J.B. Guan, B. Chen, Y.Y. Sun, H. Liang, Q.J. Zhang, J. Non-Cryst. Solids 351 (2005) 849.
[17] S. Biju, D.B. Ambili Raj, M.L.P. Reddy, B.M. Kariuki, Inorg. Chem. 45 (2006) 10651.
[18] K.H. Drexhage, J. Lumin. 1/2 (1970) 693.
[19] K.H. Drexhage, Sci. Am. 222 (1970) 108.
[20] R.M. Amos, W.L. Barnes, Phys. Rev. B 59 (1999) 7708.
[21] P. Andrew, W.L. Barnes, Phys. Rev. B (2001) 125405.
[22] T. Hayakawa, S.T. Selvan, M. Nogami, Appl. Phys. Lett. 74 (1999) 1513.
[23] S.T. Selvan, T. Hayakawa, M. Nogami, J. Phys. Chem. B 103 (1999) 7064.
[24] H. Nabika, S. Deki, J. Phys. Chem. B 107 (2003) 9161.
[25] C. Louis, S. Roux, G. Ledoux, L. Lemelle, P. Gillet, O. Tillement, P. Perriat, Adv. Mater. 16 (2004) 2163.
[26] Y.Y. Sun, H.F. Jiu, D.G. Zhang, J.G. Gao, B. Guo, Q.J. Zhang, Chem. Phys. Lett. 410 (2005) 204.
[27] Y.Y. Sun, Z. Zheng, Q. Yan, J.G. Gao, H.F. Jiu, Q.J. Zhang, Mater. Lett. 60 (2006) 2756.
[28] T. Yamase, H. Naruke, J. Phys. Chem. B 103 (1999) 8850.
[29] G.S. Ofelt, J. Chem. Phys. 37 (1962) 511.
[30] B.R. Judd, Phys. Rev. 127 (1962) 750.
[31] W. Krupke, IEEE J. Quantum Electron. 7 (1971) 153.
[32] W. Krupke, IEEE J. Quantum Electron. 10 (1974) 450.
[33] J.P. Caird, W.T. Carnall, J.P. Hessler, J. Chem. Phys. 74 (1968) 4424.
[34] S. Kühn, U. Håkanson, L. Rogobete, V. Sandoghdar, Phys. Rev. Lett. 97 (2006) 017402.
[35] H. Mertens, J.S. Biteen, H.A. Atwater, A. Polman, Nano Lett. 6 (2006) 2622.
[36] V. Ravikumar, N. Veeraiah, B. Apparao, S. Bhuddudu, J. Mater. Sci. 33 (1998) 2659.